Research Article | Vol. 27, No. 12 | 10 Jun 2019 | OPTICS EXPRESS 16560
Optics EXPRESS

# Expansion and phase correlation of a wavelength tunable gain-switched optical frequency comb

PRAJWAL D. LAKSHMIJAYASIMHA,[1,*] ALEKSANDRA KASZUBOWSKA-ANANDARAJAH,[2] EAMONN P. MARTIN,[1] PASCAL LANDAIS,[1] AND PRINCE M. ANANDARAJAH[1]

[1]*The School of Electronic Engineering, Dublin City University, Glasnevin, Dublin 9, Ireland*
[2]*CONNECT Research Centre, Dunlop Oriel House, Trinity College Dublin, Dublin 2, Ireland*
**prajwal.doddaballapural2@mail.dcu.ie*

**Abstract:** A novel scheme for the expansion and phase correlation of a wavelength tunable gain-switched optical frequency comb (OFC) is presented. This method entails firstly combining two gain-switched OFCs and expanding them using a phase modulator. Subsequently, the phase correlation between all the comb lines is induced through four-wave mixing (FWM) in a semiconductor optical amplifier (SOA). In this article, the generation of 42 highly correlated comb lines separated by 6.25 GHz, with an optical carrier to noise ratio (OCNR) of more than 50 dB, is experimentally demonstrated. In addition, the wavelength tunability of the scheme, over 30 nm within the C band, is shown. Finally, the degree of phase correlation between comb lines is verified through RF beat tone linewidth measurements. The results show a five orders of magnitude reduction in the beat tone linewidth, due to FWM in an SOA.



## 1. Introduction

The unrelenting growth of data traffic is putting a huge strain on existing optical networks. It is expected that by 2021 the internet traffic usage will reach the zettabyte ($10^{21}$) range per year [1]. To cope with this growing capacity demand, optical networks would need to employ spectrally efficient schemes such as coherent optical orthogonal frequency division multiplexing (CO-OFDM) [2] or Nyquist WDM [3]. The current industrial solution of employing an array of lasers, to support the above-mentioned modulation techniques, would not be optimum as the wavelength of an individual laser cannot be precisely controlled. As a result, spectral guard-bands are required between channels to avoid cross-channel interference, which results in a reduced spectral efficiency. A potential alternative is to use an OFC – a source that generates multiple discrete, equally spaced wavelengths from a single device, thus capable of replacing an array of lasers. The advantage of such a solution is the fixed frequency separation between the individual comb lines, which alleviates the need for the spectral guard bands. Hence, the application of OFCs can bring significant improvements in the system spectral efficiency. Also, the fixed frequency separation between the comb lines can mitigate Kerr-based non-linear effects that occur in fibre-optic communication systems, thereby enchancing the transmission reach [4].

There are several semiconductor-based OFC generation methods, each having different pros and cons. They include mode-locked lasers (MLLs) [5], which can produce ultra-broadband combs. However, MLLs suffer from a complicated fabrication process, fixed free spectral range (FSR) (dictated by the cavity length) and exhibit relatively large optical linewidths (tens of MHz) in the passive mode locking regime [6]. Another well-established OFC generation technique involves the use of electro-optic modulators (EOMs) [7]. This solution offers a tunable FSR but suffers from bias drift and high insertion losses. Microring

#359676 https://doi.org/10.1364/OE.27.016560
Journal © 2019 Received 7 Feb 2019; revised 14 May 2019; accepted 15 May 2019; published 29 May 2019

Optics EXPRESS

resonator based OFC generation also produces a broadband comb but with the downside of strong fluctuations in amplitude and phase noise [8]. Another OFC generation technique entails the use of externally injected gain-switched lasers (EI-GSL) [9]. The attractiveness of this method stems from its simplicity (uses direct modulation), cost effectiveness and flexibility. EI-GSL OFCs feature a tunable FSR, low linewidth (transferred from the master laser), high phase coherence between all OFC lines as well as central wavelength tunability [10]. In addition, these OFCs are suitable for photonic integration [11], bringing additional benefits in terms of cost and footprint reduction. Nevertheless, the main shortcoming of the EI-GSL, arising from the limited intrinsic modulation bandwidth of a laser, is the restricted number of generated comb lines. In the past, several techniques to increase the number of comb lines generated by an EI-GSL, such as the use of a modulator [12], highly nonlinear fibre (HNLF) and dispersion compensating fibre (DCF) [9], have been reported. However, these approaches resulted in limited comb expansion, added complexity and instability, and are not suited for photonic integration. More recently, other expansion methods based on dual mode injection locking [13] or cascaded Fabry Perot (FP) lasers [14] have also been studied. Nevertheless, these techniques suffered from a poor OCNR and a limited comb expansion.

In this paper, a novel method of generating a broadband and wavelength tunable OFC is experimentally demonstrated. The technique is based on the expansion and phase correlation of the combined output of two independent EI-GSL based OFCs [9] (with 13 and 14 lines with FSRs of 6.25 GHz; FSR chosen for its compatibility with the ITU-T G.694.1 grid recommendation [15]). Results achieved demonstrate an expanded OFC consisting of 42 tones (within a 3 dB range from the spectral peak) and an OCNR of more than 50 dB. Excellent phase correlation of the lines within the expanded comb is verified by measuring a 24 Hz RF beat tone linewidth. Furthermore, the wavelength tunability of the comb over 30 nm across the C band (1529 nm-1562 nm) is presented. Since the expanded OFC is based on an EI-GSL, it features all the benefits of the technique, including FSR tunability, which makes it a very attractive solution for multiple applications such as long-haul networks, sensing, mm and THz wave generation, and arbitrary waveform generation. Its practical feasibility is further enhanced by the fact that the presented configuration can be photonically integrated as well as easily scaled by adding more parallel EI-GSL stages.

## 2. Principle of comb expansion and phase correlation

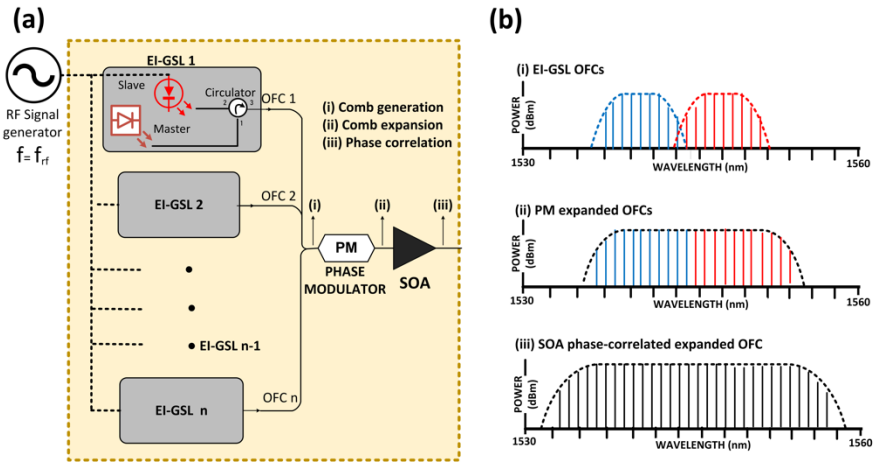


Fig. 1. (a) Block diagram of the proposed comb expansion and phase correlation technique; (b) illustration of the spectral output at each stage: (i) individual OFCs, (ii) PM output, (iii) SOA output.

Optics EXPRESS

The working principle of the proposed comb expansion and phase correlation technique is shown in Fig. 1(a). It comprises three stages: i) comb generation, ii) expansion and iii) phase correlation. The illustrative spectra of the comb at each stage are shown in Fig. 1(b). First, the OFCs are generated using the EI-GSL technique, operated in a master-slave (MS) configuration. Multiple parallel MS configurations combined together would result in an increase in the number of comb lines in the final output. In the second stage, the combined OFCs are expanded using a phase modulator to further enhance the number of comb tones. Each expanded comb portrays the phase noise properties of its master laser used for external injection [16]. Consequently, lines from different combs are not correlated in phase since injected from different master lasers. To remedy this, both combs are sent to the third stage of the set-up: phase-correlation. Here, we use an SOA operating in deep saturation to exploit its FWM-induced carrier density modulation (CDM) property. The FWM between the individual OFCs introduces a phase correlation between all the comb lines.

The fundamental aspects of the FWM effect in an SOA have been detailed in [17–20]. There are five non-linear effects responsible for FWM: carrier density modulation (CDM), carrier heating, spectral hole burning, two-photon absorption and the Kerr effect. However, CDM is the most significant FWM effect for FSRs below 100 GHz [19]. Hence, this paper focuses on the CDM effect as the OFC FSR is chosen to be 6.25 GHz.

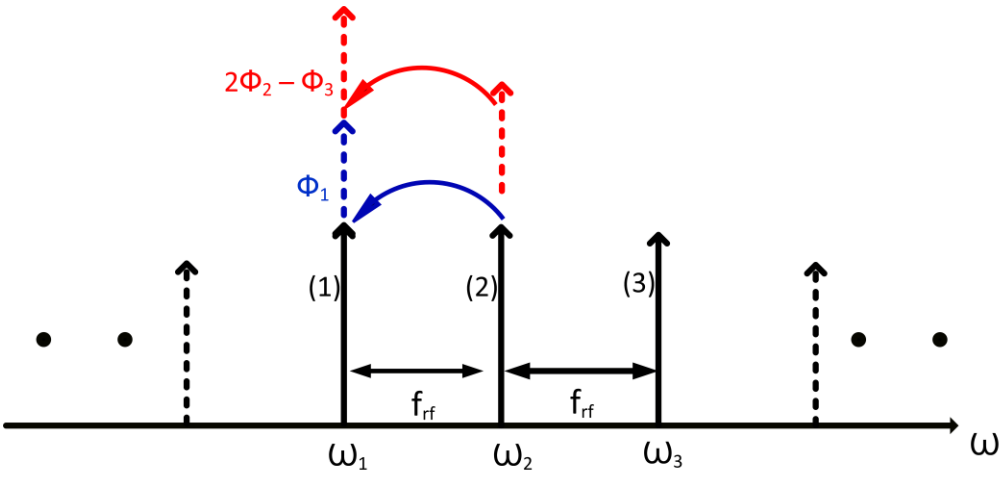


Fig. 2. Principle of phase transfer through FWM in an SOA. Here, $\varphi_1$, $\varphi_2$, $\varphi_3$ are the phases of three comb lines, respectively and $f_{rf}$ denotes the FSR of the comb. The dotted lines represent newly FWM generated spectral components.

The phase transfer phenomena, due to FWM in an SOA, is illustrated in Fig. 2. The electric field propagating through an SOA can be presented by:

$$\vec{E_i}(z,t) = A_i e^{(\omega_i t - k_i z - \varphi_i(t))}\vec{u} \tag{1}$$

where $A_i$ is the magnitude, $\omega_i$ is the angular frequency, $k_i$ is the wave vector along a given direction $\vec{u_z}$, $\varphi_i$ is the phase noise of the i[th] comb line and $\vec{u}$ is the orientation of the electric field. The contribution of the CDM to the i[th] comb line is given by [19]:

$$\delta_i^{cdm} = -\frac{1}{2}(1 - j\alpha)G_i \sum_{m=1}^{M}[\Delta N_m E_{i-m} + \Delta N_m^* E_{i+m}] \tag{2}$$

Optics EXPRESS

where $\alpha$ is the linewidth enhancement factor, $G_i$ is the linear gain, $\Delta N_m$ is the m[th] order carrier modulation and $E_i$ represents electric field of i[th] comb line. Due to the CDM, the SOA carrier population $N$, fluctuates around the average carrier density $\bar{N}$. $\Delta N_m$ is given by [21]:

$$\Delta N_m = -(N_0 - \bar{N}) \frac{\sum_{k=m+1}^{M} \frac{E_k E_{k-m}^*}{P_s}}{1 + \frac{P_t}{P_s} - jmf_{rf}\tau_e} \tag{3}$$

where $N_0$ is the average carrier number, $P_s$ is the saturation power, $P_t$ is the total power confined in the SOA waveguide, $\tau_e$ is the carrier spontaneous life time. For example, the CDM contributing to comb lines 1 and 3 are given below (for clarity we limit our analysis to 3 comb lines).

$$\delta_1^{cdm} = \frac{1}{2}(1 - j\alpha)G_1(N_0 - \bar{N})\left[\frac{|E_2|^2 E_1 + E_3^* E_2^2}{P_s + P_t - jf_{rf}\tau_e P_s}\right] \tag{4}$$

$$\delta_3^{cdm} = \frac{1}{2}(1 - j\alpha)G_3(N_0 - \bar{N})\left[\frac{|E_2|^2 E_3 + E_1^* E_2^2}{P_s + P_t - jf_{rf}\tau_e P_s}\right] \tag{5}$$

From Eq. (4), the first term in the expression of $\delta_3^{cdm}$ appears at $\omega_1$. This expression is characterised by the phase of comb line 1 $(\varphi_1)$. It corresponds to an energy transfer from comb line 2 to comb line 1. This is represented by a blue arrow in Fig. 2. The second term of $\delta_3^{cdm}$ also appears at $\omega_1 = 2\omega_2 - \omega_3$, but with the phase equal to $2\varphi_2(t) - \varphi_3(t)$, corresponding to the red arrow in Fig. 2 [21]. Similarly, the first term of $\delta_3^{cdm}$ appears at $\omega_3$, with the phase of comb line 3 $(\varphi_3)$. The second term of $\delta_3^{cdm}$ appears at $\omega_3 = 2\omega_2 - \omega_1$, with the phase equal to $2\varphi_2(t) - \varphi_1(t)$.

Therefore, the CDM contributes to the transfer of phase from comb line 2 and comb line 3 to comb line 1. The phase noise of comb line 1 is affected by these phase transfers, a process that is similar to mode locking [22].The correlation of the phase between each comb lines are realised by phase transfer due to CDM. Likewise, $\varphi_3$ is also affected by the phase transfer of $\varphi_2$ and $\varphi_1$ Thus, the phase of comb line 1 and comb line 3 become correlated. This mechanism is extended to all the comb lines that are injected into an SOA. Thus, the last stage of the proposed set-up produces a single broadband and highly coherent OFC.

## 3. Experimental setup

The experimental setup of the wavelength tunable gain-switched comb expansion and phase correlation technique is depicted in Fig. 3. Two OFCs are generated using the EI-GSL technique [9] with each OFC realised using a Master-Slave configuration. Two 200 µm long Fabry Perot (FP1 and FP2) laser diodes encased in a high-speed butterfly package are used as slave lasers (SL). The FPs, with threshold currents $(I_{th})$ of 8 and 8.5 mA, are biased at 5 × $(I_{th})$ and emit an output power of 7.7 dBm and 8.5 dBm, respectively. Two independent semiconductor-based tunable (master) lasers (TL1 and TL2) are used to inject light into the slave lasers via circulators. The power of TL1 is set to 0.5 dBm and TL2 to 1.5 dBm. This external injection enables the selection of one longitudinal mode of each of the FPs, thereby

Optics EXPRESS

achieving single mode operation at the chosen wavelengths. Polarisation controllers (PC 1 and 2) are used to align the polarisation state of the injected light with the optical waveguides of the slave lasers. Subsequently, the FPs are gain switched, by applying a 6.25 GHz electrical sinusoidal signal at a power of 24 dBm. The wavelengths of the TLs, used for the external injection, are tuned to lie on a 6.25 GHz frequency grid (19 × 6.25 GHz apart). This ensures that all lines of the two generated OFCs also appear on the same grid. The resulting OFCs are combined using a 50:50 optical coupler and temperature tuned to result in a partial overlap between them. It is observed that the overlapping of 3-4 comb lines is necessary for a strong phase transfer and the optimum spectral flatness of the expanded OFC.

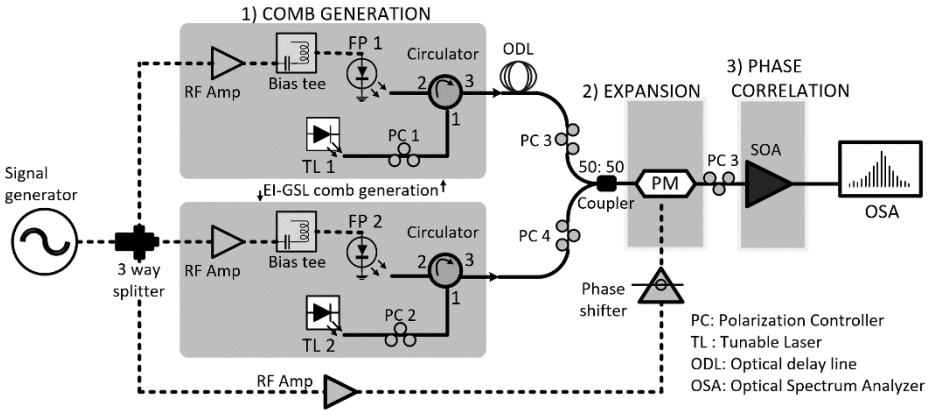


Fig. 3. Schematic of the experimental setup of the proposed wavelength tunable gain-switched comb expansion and phase correlation technique. Here, dotted lines and solid lines represent the RF and optical paths, respectively.

The combined OFCs are passed through a phase modulator (PM) to increase the number of comb lines. The insertion loss of the modulator is around 2 dB and the $V_\pi$ ~4 V at 6.25 GHz. The PM is driven by the same sinusoidal signal used for gain-switching. The amplitude of the signal is 12.5 V, which corresponds to 3.125 × $V_\pi$. The OFC expansion and flatness are optimised by aligning the RF drive modulation signal (using a phase shifter) with the gain switched optical signal (employing an optical delay line). The output signal at the PM, with an average optical power of 4.5 dBm, is injected into an SOA. The amplifier is biased at 200 mA and has a gain of 14 dB. As the maximum output power of the SOA is 14.5 dBm, the amplifier operates in deep saturation. The injected comb lines undergo FWM resulting in the generation of new spectral components at frequencies corresponding to multiples of the FSR. The interaction of the comb lines through CDM introduces a phase correlation between all the comb tones. To enhance the FWM efficiency, the state of polarisation at the input of the SOA is optimised using a polarisation controller (PC3). The SOA output is tapped using a 90:10 coupler, with 90% of the optical signal sent to an RF beat tone linewidth measurement setup (to verify the phase correlation between comb lines) and 10% recorded by a high resolution (20 MHz) optical spectrum analyser (OSA).

## 4. Results and discussion

### *4.1 Externally injected gain-switched comb generation and expansion*

The optical spectra of the free running and injection locked FP1 and FP2 lasers are shown in Figs. 4(a) and 4(b), respectively. The longitudinal mode spacing of FP1 and 2 are 1.4 nm and 1.7 nm respectively. It can be seen that the external injection enables single mode operation of the FPs, with a side-mode-suppression ratio (SMSR) > 60 dB. The spectra of the two OFCs generated by gain switching the externally injected FPs are shown in Fig. 5(a). The EI-GSL

Optics EXPRESS

OFCs consist of 13 and 14 highly coherent lines (within a 3 dB window relative to the spectral peak) and exhibit an OCNR > 50 dB. The spectra of the combined OFCs, before and after the expansion using the PM, are shown in Figs. 5(b) and 5(c), respectively. The use of the PM increases the number of generated lines from 27 to 42, while maintaining the high OCNR (>50 dB). Inducing phase correlation between the OFCs is achieved by passing the combined and expanded signal through the SOA. The resultant spectrum, shown in Fig. 5(d), clearly shows the effect of FWM, resulting in further comb expansion over 262.5 GHz. The reduced spectral flatness at this juncture could be attributed to the SOA gain response and FWM efficiency.

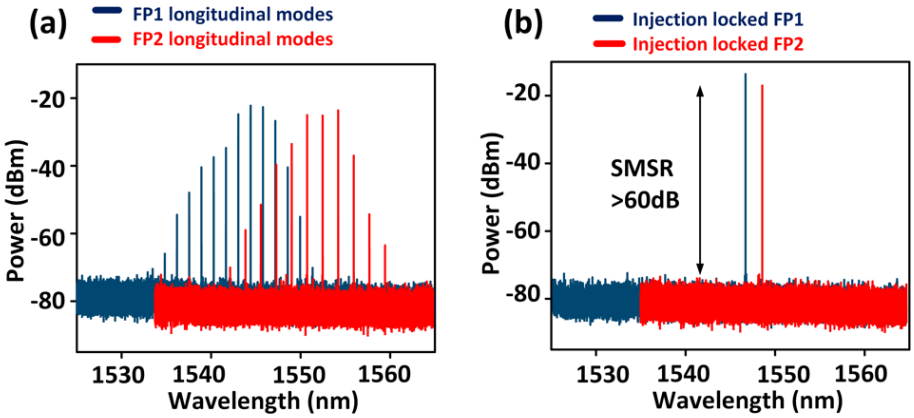


Fig. 4. Optical spectra: (a) free-running FP1 (blue) and FP2 (red), (b) externally injected FP lasers depicting single mode operation.

Optics EXPRESS

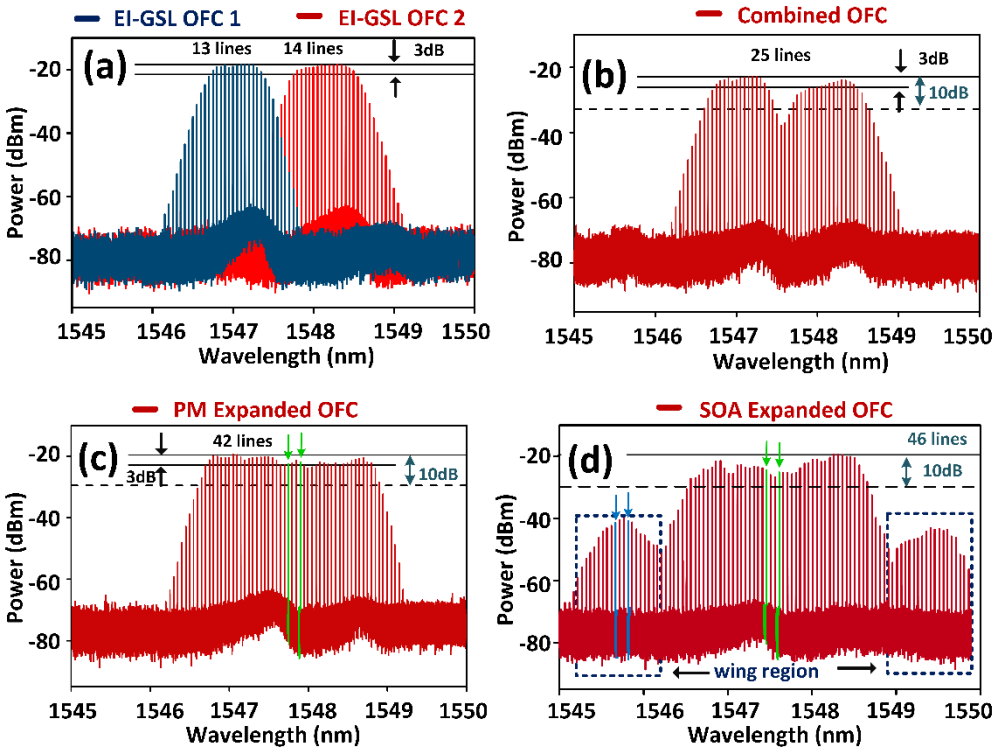


Fig. 5. Optical spectra – (a) EI-GSL OFCs where 2 OFCs are overlaid to show the amount of the overlap between the combs, (b) combined EI-GSL OFCs, (c) PM output, (d) SOA output. The pair of comb lines chosen for the RF beat tone measurements are denoted in green and blue.

It should be noted that the spectral flatness could be enhanced by optimising the entire chain (PM and SOA) rather than focusing on the output of the PM, as was done in this experiment. Improved OFC spectral flatness could also be achieved by changing the order of the devices (SOA followed by the PM). Spectral flatness optimisation techniques have not been addressed as the focus of this work is on OFC expansion and correlation.

### *4.2 Phase correlation measurement*

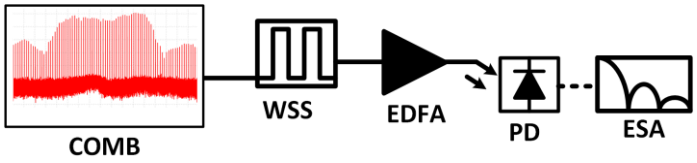


Fig. 6. RF beat tone measurement setup.

The phase correlation between the comb lines is assessed by characterising the RF beat tone linewidth. The phase correlation measurement setup is depicted in Fig. 6. A pair of comb lines are filtered using a wavelength selective switch (WSS), amplified by an Erbium doped fibre amplifier (EDFA) operating in a constant gain (15 dB) and detected by a 50 GHz photodiode. The linewidth of the resultant RF beat tone is measured with a 40 GHz electrical spectrum analyser. The beat tone linewidth is determined by the phase noise of the selected comb lines and the degree of the correlation between them. If there is no correlation between

Optics EXPRESS

the modes, the phase noise of both lines adds up, resulting in a broad RF beat tone. If the phase noise is correlated, a pure narrow RF signal is generated [23].

At first, the comb lines from individual OFCs are heterodyned on the photodetector, their phase correlation measured, and results plotted in Fig. 7(a). The beat tone linewidth is calculated to be 14 Hz, indicating excellent phase correlation. Then, two lines from the expanded OFC (after the PM), each originating from a different input comb, are chosen (marked by green lines in Fig. 5(c)). In this case the 3 dB linewidth of the RF beat tone is measured to be ~1.1 MHz, as shown in Fig. 7(b). This result is a clear indication that the phase noise of the two OFCs are uncorrelated. Subsequently, by adjusting the bandwidth of the WSS, a pair of comb lines that are frequency separated between 6.25 GHz and 37.5 GHz, upper limit set by the ESA bandwidth) and their 3 dB beat tone linewidth measured. The results are depicted Fig. 7(c) (black squares, kHz scale).

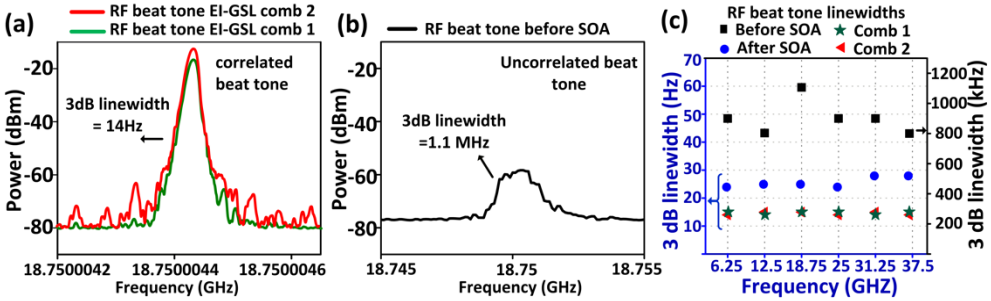


Fig. 7. Electrical spectra of RF beat tone of (a) OFC1 and OFC2 (input OFCs), (b) PM expanded OFC (uncorrelated), and (c) 3 dB linewidths of RF beat tones for different frequency separation: OFC1 (green star), OFC2 (red triangle), SOA output (blue circles) in Hz scale and PM output (black square) in kHz scale.

To validate the phase correlation due to FWM, the RF beat tone linewidth measurement is repeated on the output signal of the SOA. For this test we choose comb lines from the wings of the spectrum (denoted by the dotted rectangle in Fig. 5(d)) that were generated in the SOA. By doing so, we ensure that the measurement is carried out on lines originating from different combs. These spectral components arise from the FWM of the two independent OFCs in the SOA. Verification of the latter was achieved by passing one OFC at a time through the SOA. The two resultant spectra (blue and red combs) are recorded and shown in Figs. 8(a) and 8(b). From the figure it can be seen that the afore-mentioned wings are only present if both OFCs are passing through the SOA. The 3 dB RF beat tone linewidth of the FWM generated lines (blue tones in Fig. 5(d)) was found to be ~24 Hz, as seen in Fig. 9 (inset, blue trace). In addition, the beat tones of comb lines, separated by frequencies between 6.25 GHz and 37.5 GHz, are measured and the results plotted in Fig. 7(c) (blue circles). The huge improvement in the beat tone linewidth, between the input and output of the SOA, (reduction from 1.1 MHz to 24 Hz, Fig. 9), proves that the FWM induces a phase correlation between all the comb lines. It can also be seen that the beat tone linewidth of the expanded and correlated comb is only slightly larger than that of the individual input combs (24 Hz vs. 14 Hz). This might be attributed to the FWM efficiency.

Optics EXPRESS

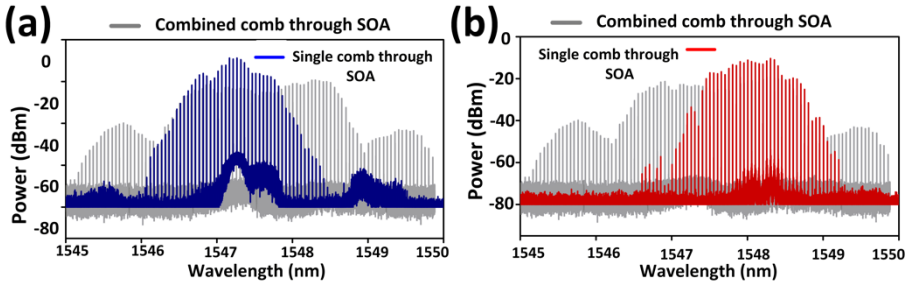


Fig. 8. Optical spectra of the SOA output of the individual expanded OFCs: (a) OFC1 (blue) and (b) OFC2 (red). The combined expanded SOA output (grey, Fig. 5(c)) is superimposed for comparison.

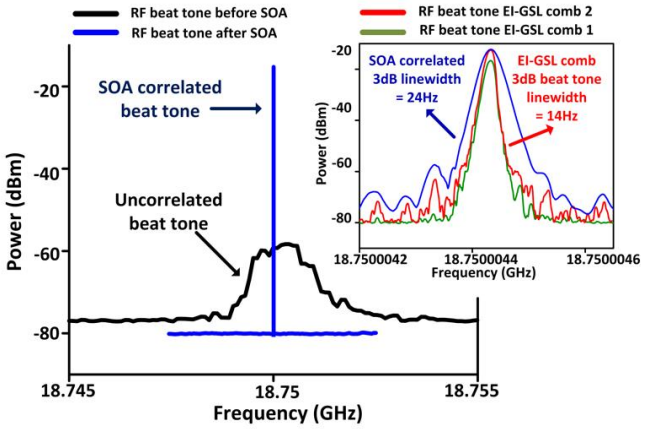


Fig. 9. Electrical spectra for RF beat tone of two comb lines: uncorrelated (SOA input, black trace), correlated (SOA output, blue trace). Inset: zoom in on the RF beat tone of the individual input OFCs and the expanded + phase correlated OFC at the SOA output.

### *4.3 Central emission wavelength tunability*

The proposed comb expansion and correlation technique also offers wavelength tunability, across the entire C band. Wavelength tuning can be achieved by injecting light from the master laser (TL) into different longitudinal modes of each of the gain-switched slave (FP) lasers, thus generating combs at different wavelengths. To demonstrate it, two additional wavelength operating points were tested. Figures 10(a) – (c) shows the comb spectra at different stages of the set-up, when the expanded comb is centred at 1560 nm, while plots Figs. 10(d) – (f) illustrate the spectra of the comb centred around 1531 nm. Once again, the increase in the total number of lines, due to the use of PM, is clearly visible: from 29 to 43 lines at 1560 nm and from 19 to 30 lines at 1531 nm. Passing these combs through the SOA results in a further spectral growth but degrades the overall spectral flatness.

Optics EXPRESS

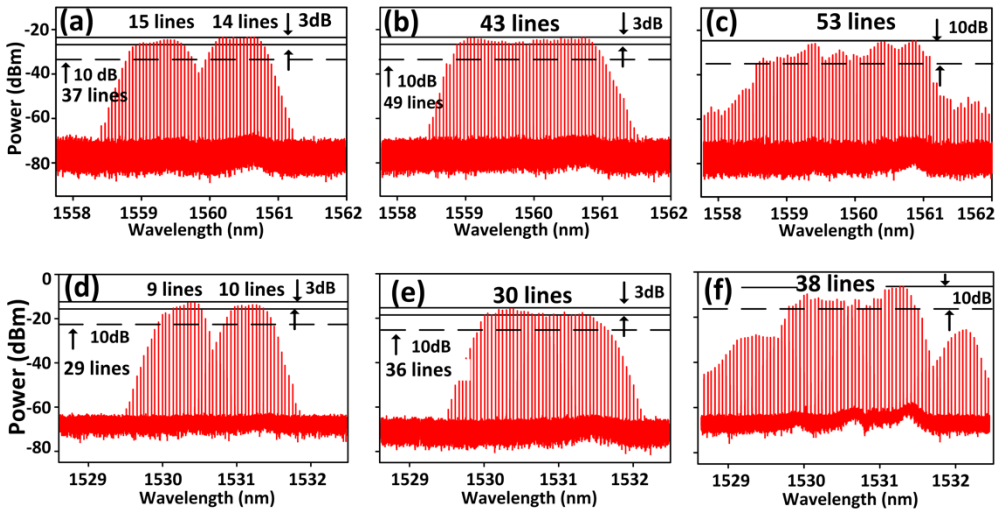


Fig. 10. Optical spectra demonstrating wavelength tunability of the proposed configuration: (a) combined EI-GSL OFCs, (b) PM output, (c) SOA expansion at 1560nm; (d) combined EI-GSL OFCs, (e) PM output and (f) SOA expansion at 1531nm.

## 5. Conclusion

A novel method of wavelength tunable comb expansion and phase correlation has been experimentally investigated. The proposed scheme is capable of generating a broadband OFC consisting of 42 clearly resolved, phase correlated lines with an FSR of 6.25 GHz and with an OCNR larger than 50 dB. The concept of inducing a phase correlation between all the comb lines through FWM has been proven by measuring the RF beat tone linewidth. The results show a five-order magnitude reduction in the beat tone linewidth (1.1 MHz to 24 Hz) and confirm the high degree of phase correlation achieved. Furthermore, this correlation is maintained for all measured beat tone frequencies (from 6.25 GHz to 37.5 GHz). The wavelength tunability of the scheme, by generating the extended OFC at wavelengths between 1529 – 1562 nm, has also been demonstrated. Finally, the proposed scheme can be photonically integrated and easily scaled by adding more input OFCs in parallel.

In summary, the proposed comb generator, enabling simple and cost-efficient generation of tones with precisely controlled channel spacing, narrow linewidth and a high degree of phase correlation, will be an asset in the realisation of the next generation terabit networks employing high spectral density modulation formats.

## Funding

Science Foundation Ireland (SFI) via the Career Development Award (SFI 15/CDA/3640), SFI/European Regional Development Fund (13/RC/2077), SFI Industry Fellowship Award 17/IFB/5385, 12/RC/2276 and 16/RI/3698.

## References

1. Cisco, Visual Networking Index white paper "The Zettabyte Era: Trends and Analysis," (2017).
2. G. Zhang, M. De Leenheer, A. Morea, and B. Mukherjee, "A survey on OFDM-based elastic core optical networking," IEEE Comm. Surv. and Tutor. **15**(1), 65–87 (2013).
3. G. Bosco, V. Curri, A. Carena, P. Poggiolini, and F. Forghieri, "On the performance of nyquist-WDM terabit superchannels based on PM-BPSK, PM-QPSK, PM-8QAM or PM-16QAM subcarriers," J. Lightwave Technol. **29**(1), 53–61 (2011).
4. N. Alic, E. Myslivets, E. Temprana, B. P. Kuo, and S. Radic, "Nonlinearity Cancellation in Fiber Optic Links Based on Frequency Referenced Carriers," J. Lightwave Technol. **32**(15), 2690–2698 (2014).
5. S. Latkowski, F. Surre, R. Maldonado-basilio, and P. Landais, "Investigation on the origin of terahertz waves generated by dc-biased multimode semiconductor lasers at room temperature," Appl. Phys. Lett. **93**(24), 241110

Optics EXPRESS

(2008).
6. T. Habruseva, S. O'Donoghue, N. Rebrova, F. Kéfélian, S. P. Hegarty, and G. Huyet, "Optical linewidth of a passively mode-locked semiconductor laser," Opt. Lett. **34**(21), 3307–3309 (2009).
7. M. Fujiwara, J. Kani, H. Suzuki, K. Araya, and M. Teshima, "Flattened optical multicarrier generation of 12.5 GHz spaced 256 channels based on sinusoidal amplitude and phase hybrid modulation," Electronics Lett. **37**(15), 967–968 (2000).
8. P. Del'Haye, O. Arcizet, A. Schliesser, R. Holzwarth, and T. J. Kippenberg, "Full stabilization of a microresonator-based optical frequency comb," Phys. Rev. Lett. **101**(5), 053903 (2008).
9. P. M. Anandarajah, R. Maher, Y. Q. Xu, S. Latkowski, J. O'carroll, S. G. Murdoch, R. Phelan, J. O'Gorman, and L. P. Barry, "Generation of coherent multicarrier signals by gain switching of discrete mode lasers," IEEE Photonics J. **3**(1), 112–122 (2011).
10. P. M. Anandarajah, R. Zhou, R. Maher, M. D. G. Pascual, F. Smyth, V. Vujicic, and L.P. Barry, "Flexible Optical Comb Source for Super Channel Systems," in 2013 Optical Fiber Communication Conference and Exposition and the National Fiber Optical Engineers Conference (IEEE, 2013), paper OTh3I.8.
11. R. Zhou, P. M. Anandarajah, M. D. G. Pascual, J. O'Carroll, R. Phelan, B. Kelly, and L. P. Barry,"Monolithically integrated 2-section lasers for injection locked gain switched comb generation," in Optical Fiber Communication Conference and Exposition (Optical Society of America, 2014), paper Th3A.3.
12. R. Zhou, S. Latkowski, J. O'Carroll, R. Phelan, L. P. Barry, and P. Anandarajah, "40 nm wavelength tunable gain-switched optical comb source," Opt. Express **19**(26), B415–B420 (2011).
13. M. D. G. Pascual, R. Zhou, F. Smyth, T. Shao, P. M. Anandarajah, and L. Barry, "Dual mode injection locking of a Fabry-Pérot laser for tunable broadband gain switched comb generation," in 2015 European Conference on Optical Communication (IEEE, 2015), pp. 1–3.
14. M. D. G. Pascual, P. M. Anandarajah, R. Zhou, F. Smyth, S. Latkowski, and L. P. Barry, "Cascaded Fabry-Perot lasers for coherent expansion of wavelength tunable gain switched comb," in 2014 European Conference on Optical Communication (IEEE, 2014), pp. 1–3.
15. International Telecommunications Union-Telecommunication Standardization Sector, *ITU-T Recommendation G.694.1: Spectral grids for WDM applications: DWDM frequency grid* (UTI-T, 2012), pp. 1–16.
16. R. Zhou, T. N. Huynh, V. Vujicic, P. M. Anandarajah, and L. P. Barry, "Phase noise analysis of injected gain switched comb source for coherent communications," Opt. Express **22**(7), 8120–8125 (2014).
17. S. Diez, C. Schmidt, R. Ludwig, H. G. Weber, K. Obermann, S. Kindt, I. Koltchanov, and K. Petermann, "Four-wave mixing in semiconductor optical amplifiers for frequency conversion and fast optical switching," IEEE J. Sel. Top. Quantum Electron. **3**(5), 1131–1145 (1997).
18. O. Aso, M. Tadakuma, and S. Namiki, "Four-wave mixing in optical fibers and its applications," Furukawa Rev. **19**(19), 63–68 (2000).
19. G. P. Agrawal, "Population pulsations and nondegenerate four-wave mixing in semiconductor lasers and amplifiers," J. Opt. Soc. Am. B **5**(1), 147–159 (1988).
20. G. P. Agrawal, "Highly nondegenerate four-wave mixing in semiconductor lasers due to spectral hole burning," Appl. Phys. Lett. **51**(5), 302–304 (1987).
21. J. Renaudier, G. H. Duan, P. Landais, and P. Gallion, "Phase correlation and linewidth reduction of 40 GHz self-pulsation in distributed Bragg reflector semiconductor lasers," IEEE J. Quantum Electron. **43**(2), 147–156 (2007).
22. K. A. Shore and W. M. Yee, "Theory of self-locking FM operation in semiconductor lasers," IEE Proc. J. Optoelectronics **138**(2), 91–96 (1991).
23. K. Kikuchi, "Characterization of semiconductor-laser phase noise and estimation of bit-error rate performance with low-speed offline digital coherent receivers," Opt. Express **20**(5), 5291–5302 (2012).